

1 **Oceland: A conceptual model for ocean-land-atmosphere interactions based**  
2 **on water balance equations**

3 Luca Schmidt<sup>a</sup>, Cathy Hohenegger<sup>a</sup>

4 <sup>a</sup> *Max Planck Institute for Meteorology, Hamburg*

5 *Corresponding author:* Luca Schmidt, [luca.schmidt@mpimet.mpg.de](mailto:luca.schmidt@mpimet.mpg.de)

6 ABSTRACT: The spatial distribution of precipitation is often misrepresented by General Cir-  
7 culation Models (GCM). In particular, precipitation tends to be underestimated over land and  
8 overestimated over ocean. One obstacle to resolving this longstanding issue is the lack of a general  
9 understanding of land-ocean-atmosphere interactions. More precisely, we do not have a funda-  
10 mental theory that tells us which processes or physical quantities determine the partitioning of  
11 precipitation between land and ocean. In this study, we investigate whether large-scale constraints  
12 on this partitioning exist by using a conceptual box model based on water balance equations. With  
13 a small number of empirical but physically motivated parametrizations of the water balance com-  
14 ponents, we construct a set of coupled ordinary differential equations which describe the dynamical  
15 behaviour of the water vapour content of land and ocean atmospheres as well as the soil moisture  
16 content of land. We compute the equilibrium solution of this land-ocean-atmosphere system and  
17 analyze the sensitivity of the equilibrium state to model parameter choices. The results show that  
18 the ratio of mean land and ocean precipitation rates is primarily controlled by a scale-dependent  
19 atmospheric moisture transport parameter, the land fraction, and the permanent wilting point of  
20 the soil. We further demonstrate how the proposed model can be adapted for applications on  
21 both global and local scales to model, where the latter is useful to study e.g. island precipitation  
22 enhancement. For a global scale model configuration with one ocean and one land domain, we  
23 show that the precipitation ratio is constrained to a range between zero and one and are able to  
24 explain this behavior based on the underlying equations and the fundamental property of land to  
25 loose water through runoff.

## 26 1. Introduction

27 As human beings, we have a great interest in how Earth's climate and its change over time  
28 influence living conditions on the land surface. An important question in this respect is how  
29 much of the water that evaporates from the Earth's surface will precipitate over land as opposed  
30 to over the ocean. Unfortunately, even sophisticated General Circulation Models frequently fail to  
31 reproduce observed spatial patterns of precipitation, especially in the Tropics where precipitation  
32 amounts are high [Fiedler et al. (2020) and references therein]. However, more fundamentally,  
33 we are lacking a theoretical framework in which the partitioning of precipitation between land  
34 and ocean can be explained and analyzed with respect to its dependence on properties of the  
35 system which may or may not change over time. For instance, is the partitioning sensitive to land  
36 size? Do surface characteristics such as soil type matter or is it rather atmospheric conditions that  
37 dominate the behavior? It is the aim of this study to introduce a conceptual water balance model  
38 that reduces the complexity of the real world to a small number of physical processes that are key  
39 for understanding the precipitation partitioning. By investigating the sensitivity of the modelled  
40 precipitation partitioning to a variation of the model parameter values, this study can serve as a  
41 starting point for filling the gap of theoretical understanding described above.

42 Traditionally, hydrologists separate the Earth's hydrological cycle into an atmospheric branch,  
43 describing the sinks and sources of atmospheric moisture, and a terrestrial branch, describe the  
44 change of soil moisture [e.g.  
45 Peixóto and Oort (1983)]. Evapotranspiration (ET) and precipitation are the links that connect the  
46 two branches of the cycle. Since we aim at understanding the precipitation partitioning between  
47 land and ocean, it is convenient to choose a different perspective and think about an ocean and  
48 a land branch of the water cycle instead. The land and ocean branches are then linked through  
49 advective moisture transport between land and ocean atmospheres, and through runoff from the  
50 soil to the ocean.

51 The land branch in isolation has been studied intensively since the 1950s. In a pioneering  
52 land-atmosphere interaction study by Budyko and Drozdov (1953), the authors describe how an  
53 airstream that traverses a region imports atmospheric moisture at the windward contour, moistens  
54 or dries depending on the relative magnitude of mean precipitation and ET, and exports moisture at  
55 the leeward contour. In this one-dimensional framework known as the Budyko model, precipitation

56 in the region can be expressed as a sum of two components: water that is advected from outside  
57 the region and water that previously evaporated from the surface inside the region. The relative  
58 contribution of the two components to total precipitation and, hence, the dependence of regional  
59 precipitation on advected moisture relative to local recycling through ET, can be expressed as a  
60 water recycling coefficient. Important studies that used observations to estimate the water balance  
61 components and compute recycling coefficients include Brubaker et al. (1993), who formulated a  
62 two-dimensional Budyko model and investigated precipitation recycling in four innercontinental  
63 areas and Eltahir and Bras (1994), who focused on the Amazon region and refined the 2D model  
64 by allowing for a horizontally heterogeneous precipitation and evapotranspiration field (see Burde  
65 and Zangvil (2001) for a comprehensive review of the different adaptations of Budyko's framework  
66 and their limitations). A shortcoming of most recycling studies is the dependence of recycling  
67 coefficients on the size of the region of interest. The larger the region, the more precipitating  
68 water will be derived from within the region. Ent et al. (2010) circumvented this problem by  
69 taking a global perspective and defining recycled water as previously evaporated from any point  
70 on the land surface and advected water as evaporated from any point on the ocean surface. All  
71 mentioned studies show that precipitation recycling contributes significantly to land precipitation,  
72 especially in hotspot regions of land-atmosphere interactions such as the Sahel region, the Amazon  
73 or mountainous regions in Asia.

74 An alternative to estimating the water balance components from observations is to use analytical  
75 parametrizations. In water-limited areas, ET is a function of soil moisture as described by e.g.  
76 Manabe (1969) or more recently updated in Seneviratne et al. (2010). Applied to the Budyko  
77 recycling framework, this turns the total precipitation into a function of soil moisture, mean  
78 advected precipitation, domain size and environmental parameters such as wind speed and potential  
79 evapotranspiration. The variability of the latter parameters introduces considerable randomness  
80 of precipitation in the real world and limits the utility of the Budyko model when being fixed to  
81 constant values. Rodriguez-Iturbe et al. (1991) and Entekhabi et al. (1992) address this issue by  
82 modulating mean parametric environmental conditions with Gaussian white noise. Both found  
83 that the system preferentially resides in a very dry or very moist soil moisture state for sufficiently  
84 high amplitudes of environmental variability. This finding suggests that even such a simple model  
85 offers an explanation for hydrological extremes such as droughts in continental regions.

86 What are the physical mechanisms that makes precipitation soil moisture-dependent? Broadly  
87 speaking, two lines of arguments were developed. The first one predicts a mostly positive feedback  
88 between precipitation and soil moisture, arguing that the enhanced latent heat flux over wet soils  
89 favors precipitating convection either through direct water input that can be recycled [e.g. Zangvil  
90 et al. (1993)] or by destabilizing the vertical profile in the air aloft [Schär et al. (1999), Findell and  
91 Eltahir (2003)]. Hohenegger et al. (2009) points out that the sign of this feedback mechanism can  
92 depend on model resolution and the choice of parametrization schemes. The second line of argu-  
93 ment explains the soil moisture-precipitation feedback through mesoscale circulations that develop  
94 due to different Bowen ratios of wet and dry soil patches Segal and Arritt (1992). Such circulations  
95 may drive convective systems from rather moist to rather dry surface areas and contribute to a  
96 homogenization of soil moisture [Lynn et al. (1998), Hohenegger and Stevens (2018)]. However,  
97 Froidevaux et al. (2014) found that synoptic background winds can also displace convective air  
98 from drier soils, where convection was initiated, to wetter soils where the atmospheric conditions  
99 favor the onset of precipitation. Hence, the sign of the soil moisture feedback related to mesoscale  
100 processes is unclear.

101 The circulation argument has direct implications for our initial question about precipitation  
102 partitioning between land and ocean. In the context of Tropical islands, several studies showed that  
103 precipitation is enhanced over land due to sea breezes induced by daytime differential heating [Qian  
104 (2008), Cronin et al. (2015)]. Even though island precipitation enhancement is often associated  
105 with energy balance arguments which are not considered in this work, other factors such as island  
106 size [Sobel et al. (2011), Cronin et al. (2015), Wang and Sobel (2017), Ulrich and Bellon (2019)]  
107 and background wind speed [Sobel et al. (2011), Wang and Sobel (2017)] seem to matter, too, and  
108 these factors might be independent of the occurrence of sea breezes. We will return to the case of  
109 islands in the last part of this paper and explore what a purely water balance based approach can  
110 teach us about precipitation enhancement in such small-scale systems.

## 111 **2. Model description**

112 In this study, we want to understand the controlling factors for precipitation partitioning between  
113 land and ocean. Specifically, we ask whether fundamental constraints for this partitioning arise  
114 from water balance equations. To this end, we propose a box model as sketched in Figure 1 with

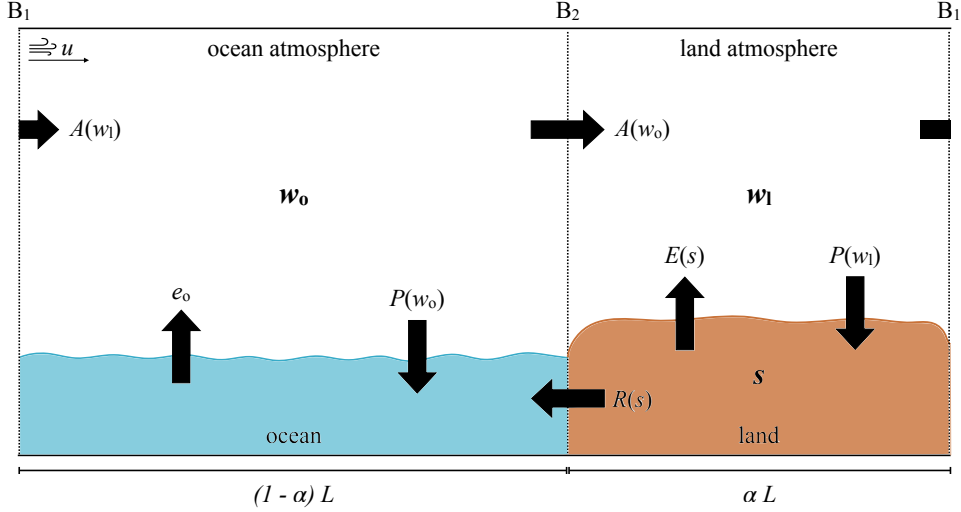


FIG. 1. Closed model sketch and water vapor pass distribution.

115 an ocean domain, denoted by subscript ‘o’, and a land domain, denoted by subscript ‘l’. The  
 116 relative size of the two domains is given by the land fraction parameter  $\alpha$ . Each of the two domains  
 117 contains a ground box at the bottom (ocean or land) and an atmospheric box aloft. While the  
 118 horizontal extent of the model is prescribed by length  $L$ , the downward/upward vertical extent of  
 119 the ground/atmospheric boxes is taken to be infinite. The model has periodic boundary conditions,  
 120 i.e. topologically, it resembles the wall of a cylinder with the right boundary of the land domain  
 121 connecting to the left boundary of the ocean domain. This turns the model into a closed system  
 122 in which water is conserved and which does not interact with any external environment. Such a  
 123 *closed* model (CM) can be used to describe, for example, the entire globe or the full Tropics if  
 124 net water exchange with the Extratropics can be assumed to be negligible. Later, in section 5, we  
 125 introduce an *open* model (OM) formulation suitable for regional systems in which case boundary  
 126 values are provided by synoptic-scale conditions and the modelled area can act as a net sink or  
 127 source of moisture. In this case, water is still conserved in a global sense but not necessarily within  
 128 the model.

#### 129 a. Water balance equations

130 We further assume that the model boxes have well-mixed properties and that all water fluxes  
 131 between them can be expressed as functions of their mean moisture content, i.e. the moisture state

of the boxes. For atmospheric boxes, we use the mean integrated water vapour pass  $w$  in mm, and for the land box the unitless mean relative soil moisture saturation  $s$  to describe the moisture state. As the ocean is considered fully saturated at all times, we don't need to assign a moisture variable to it. Hence, the full information on the moisture state of the model at any given moment in time  $t$  is given by the set of state variables  $\{w_o(t), w_l(t), s(t)\}$ .

Following earlier studies by Peixóto and Oort (1983) and Brubaker et al. (1991), we describe the time-evolution of the state variables by coupled water balance equations in which moisture sinks and sources are represented by water fluxes between the boxes:

$$\frac{ds}{dt} = \frac{1}{nz_r} [P(w_l) - R(s, w_l) - E(s)] \quad (1)$$

$$\frac{dw_l}{dt} = E(s) - P(w_l) + A_l(w_l, w_o) \quad (2)$$

$$\frac{dw_o}{dt} = e_o - P(w_o) + A_o(w_l, w_o). \quad (3)$$

The relevant fluxes, which are indicated by black arrows in Figure 1, are precipitation  $P$  from atmosphere to ground boxes, evapotranspiration  $E$  from soil to land atmosphere, ocean evaporation  $e_o$  to the ocean atmosphere, runoff  $R$  from soil to ocean and advection  $A$  between the atmospheric boxes. All fluxes are given as spatio-temporal mean flux rates in mm/day ('mean' being frequently omitted in the remainder of this text). This is, in order to obtain the total moisture change in mm<sup>2</sup>/day, Equations (1) and (2) would need to be multiplied by land domain size  $\alpha L$  and Equation (3) by ocean domain size  $(1 - \alpha)L$ . The advection terms  $A_l$  and  $A_o$  refer to the *net* advection rate into the land and ocean atmosphere, respectively, and are positive for a net moisture import and negative for net moisture export. Dimensionless soil porosity  $n$ , hydrologically active soil depth  $z_r$  in mm and  $e_o$  are constant model parameters. An implicit assumption of this water balance approach is that the water holding capacity of the atmosphere does not change significantly over long enough timescales which we consider here.

## b. Parametrizations

While the conservation of water is a rather fundamental condition, there are no simple fundamental laws governing the water fluxes between the model boxes. Instead, we need to turn to empirical

relationships between the flux quantities and moisture state variables, as has been previously done by Rodriguez-Iturbe et al. (1991). We adopt their parametrization of runoff as the fraction  $R_f$  of precipitation that does not infiltrate the soil but instead returns to the ocean in the form of surface or sub-surface currents. The runoff fraction,

$$R_f(s) = \epsilon s^r, \quad (4)$$

contains two empirical dimensionless parameters  $\epsilon \approx 1$  and  $r \approx 2$ . It tells us that runoff intensifies as the soil moistens. The complete expression for the runoff rate reads

$$R(s, w_1) = R_f(s)P(w_1), \quad (5)$$

but it proves to be convenient to combine precipitation and runoff in Eqn. (1) to  $P(w_1) - R(s, w_1) = P(w_1)\Phi(s)$ , where we introduced the infiltration function  $\Phi(s) = 1 - R_f = 1 - \epsilon s^r$ . Note, that this parametrisation assumes that runoff discharge happens uniformly across the land domain and that its water does not participate in any secondary processes that could moisten the soil.

For precipitation, Rodriguez-Iturbe et al. (1991) follow the approach by Budyko and Drozdov (1953) and obtain an expression for precipitation that is dependent on soil moisture. However, the Budyko approach assumes the advected precipitation component to be known and set to a fixed value which is not a desirable construction in our case where precisely the interaction of land and ocean through advection is one main focus. Instead, we use the empirical parametrization established by Bretherton et al. (2004). The authors find that the precipitation rate over tropical oceanic regions shows an exponential relationship with the mean water vapor pass,

$$P(w) = \exp \left[ a \left( \frac{w}{w_{\text{sat}}} - b \right) \right]. \quad (6)$$

The parametrization introduces three parameters, two empirical dimensionless parameters  $a \approx 15.6$  and  $b \approx 0.6$  and the saturated water vapor pass  $w_{\text{sat}}$  in mm. Lacking a corresponding expression for extratropical ocean regions and land in general, we make the explicit assumption that Equation (6) can also be applied to all atmospheres. This assumption is rather crude and has major implications for the results presented in Section 4 as will be discussed in greater detail later. Furthermore, the



177 same saturation water vapor pass is assumed over land and over ocean, implying similar energetic  
 178 conditions across the entire model domain.

179 The qualitative dependence of evapotranspiration (ET) on soil moisture saturation is long-known,  
 180 see e.g. Budyko (1956) or more recently and slightly modified in Seneviratne et al. (2010). ET  
 181 is close to zero for soil moisture saturation values below the permanent wilting point,  $s < s_{\text{pwp}}$ ,  
 182 increases approximately linearly in a transition range between the permanent wilting point and a  
 183 critical value close to the field capacity,  $s_{\text{pwp}} < s < s_{\text{fc}}$  and reaches a plateau for higher  $s$ -values,  
 184  $s > s_{\text{fc}}$ , where evapotranspiration is nearly constant. The evapotranspiration value of the plateau  
 185 is denoted by  $E_p$ . It is an energy-dependent parameter that increases with increasing radiative  
 186 energy input. In this work,  $E_p$  will be set to a constant value. For computational convenience,  
 187 we parametrize evapotranspiration by the following smooth function which has the qualitative  
 188 properties described above,

$$E(s) = \frac{E_p}{2} \left[ \tanh \left( 10 \left( s - \frac{s_{\text{pwp}} + s_{\text{fc}}}{2} \right) \right) + 1 \right]. \quad (7)$$

189 This parametrization implies that the entire land box is either covered by a single vegetation type  
 190 or that a combination of vegetation types can be modelled by means of an effective mean value of  
 191  $s_{\text{pwp}}$ ,  $s_{\text{fc}}$  and  $E_p$ .

192 It remains to find expressions for the *mean net* advection rates into the land and ocean atmospheres,  
 193 hereafter just land/ocean advection rates. The net total advection flux into a given box is the  
 194 difference between the moisture entering and leaving the box per unit time. This moisture transport  
 195 is driven by a mean background wind velocity  $u$  which we assume to be constant across the model  
 196 domain. Total advection in  $\text{mm}^2/\text{day}$  can then be expressed as

$$A_{\text{tot}} = (w_{\text{in}} - w_{\text{out}})u. \quad (8)$$

197 The assumed water vapour pass distribution is characterized by one value  $w_o$  across the ocean  
 198 atmosphere and another value  $w_l$  across the land atmosphere. Hence, wind transports the moisture  
 199 amount  $w_o u$  into the land domain and  $w_l u$  into the ocean domain. Since we only have two boxes  
 200 and periodic boundary conditions, the total net advection rate  $A_{\text{tot}}$  into the land and ocean domains  
 201 are identical in magnitude but with opposite signs. If the ocean has a net advective outflux, then

TABLE 1. Parameter ranges for closed model Monte Carlo simulations with uniform sampling.

Parameter	Minimum	Maximum	Range choice motivated by
$s_{\text{pwp}}$	0.2	0.54	Hagemann and Stacke (2015)
$s_{\text{fc}}$	0.5	0.84	Hagemann and Stacke (2015)
$e_{\text{p}}$ [mm/day]	4.1	4.5	Rodriguez-Iturbe et al. (1991)
$nZ_{\text{r}}$ [mm]	90.0	110.0	Rodriguez-Iturbe et al. (1991)
$e_{\text{o}}$ [mm/day]	2.8	3.2	C. Hohenegger, private communications
$\epsilon$	0.9	1.1	Rodriguez-Iturbe et al. (1991)
$r$	2.0	2.0	fixed due to computational method, Rodriguez-Iturbe et al. (1991)
$a$	11.4	15.6	Bretherton et al. (2004)
$b$	0.522	0.603	Bretherton et al. (2004)
$w_{\text{sat}}$ [mm]	65.0	80.0	Bretherton et al. (2004)
$\alpha$	0.0	1.0	full possible range
$u$ [m/s]	1.0	10.0	reasonable range for lower tropospheric mean wind speed
$L$ [km]	1000.0	40000.0	chosen to represent different length scales
$\tau = u/L$ [day $^{-1}$ ]	0.00216	0.864	computed from extreme $u$ and $L$

the land atmosphere gains this moisture as net advective influx. In a last step, this total advection rate needs to be translating into *mean* advection rates per unit land/ocean length, i.e.

$$A_1 = \frac{(w_o - w_l)u}{\alpha L} \quad (9)$$

and

$$A_o = -\frac{(w_o - w_l)u}{(1 - \alpha)L}, \quad (10)$$

where  $A_1$  and  $A_o$  have units mm/day and  $\alpha$  and  $L$  are the land fraction and full model length, respectively, as introduced earlier.

With these parametrizations, the model has a total of 14 free parameters which we can reduce to 12 if we treat  $nZ_r$  in mm as one combined parameter and introduce  $\tau = u/L$  in day $^{-1}$  as a characteristic rate of atmospheric transport. Table 1 provides sensible ranges for the 12 parameters. These ranges are used to constrain the precipitation ratio across the parameter space and test the sensitivity of the model results to parameter variations.

### 3. Evaluation methods

In this section, we present the analysis methods that are employed to evaluate the model behavior and assess the sensitivity of the precipitation ratio to a variation of the model parameters.

215 The focus of the present study lies on the properties of equilibrium states of the modelled system.  
 216 The equilibrium solution to the model equations (1) to (3) has to be found numerically. We use  
 217 the `DynamicalSystems.jl` library from Datseris (2018) to find all roots of the model equations  
 218 and determine whether each root represents a stable or unstable fixed point of the system. With  
 219 the equilibrium soil moisture and water vapour pass values obtained in this way, we can compute  
 220 all fluxes and flux ratios of interest using the parametrizations introduced in Section 2.b.

221 Adopting an agnostic view on the plausibility of each combination of parameter values from the  
 222 ranges given in Tab. 1, we are confronted with a 12-dimensional parameter space with uniform  
 223 probability distribution. A general assessment of the sensitivity of equilibrium states and related  
 224 quantities to a variation of the model parameters requires a sampling of the full parameter space. To  
 225 this end, we perform  $n = 10000$  model simulations for randomly chosen combinations of parameter  
 226 values, each yielding a corresponding fixed point.

227 Having obtained a sufficiently large dataset in this way, the sensitivity of a computed quantity  $Q$   
 228 such as the precipitation ratio to a given parameter  $p$  can be visually and quantitatively evaluated  
 229 with  $Q$ - $p$  scatter plots. The sensitivity is given by the correlation between  $Q$  and corresponding  $p$   
 230 values. For a potentially non-linear and non-monotonic distribution of the data points, a suitable  
 231 sensitivity measure is the mutual information  $MI(p, Q)$  which quantifies how much knowing the  
 232 value of  $p$  will reduce the uncertainty about  $Q$ . Mutual information  $MI$  is computed as,

$$MI(p, Q) = H(p) + H(Q) - H(p, Q), \quad (11)$$

233 where  $H(p)$ ,  $H(Q)$  and  $H(p, Q)$  are the information entropies [Shannon (1948)] of  $p$  and  $Q$  values  
 234 and their joint distribution, respectively, where we use amplitude binning to ascribe probability  
 235 distributions. We follow an approach by Datseris and Parlitz (2022) to assess the significance level  
 236 for an obtained sensitivity value and to compare the sensitivity of different parameters  $p_i$ . To this  
 237 end, we define a mutual information index

$$I_{MI}(p_i) = \frac{MI(\hat{p}_i, Q)}{MI_{\text{uncorr}, 3\sigma}(\hat{p}_i, Q)}, \quad (12)$$

238 where  $\hat{p}_i$  denotes a rescaled version of  $p_i$  with values between 0 and 1 and  $MI_{\text{uncorr}, 3\sigma}(\hat{p}_i, Q)$   
 239 is the mutual information value that deviates by three standard deviations  $\sigma$  from the mean of

a distribution of  $MI$  values for uncorrelated  $\hat{p}_i$  and  $Q$ . A detailed description of this method is presented in Appendix [\*\*\*].  $I_{MI} = 1$  is used as the significance threshold and the higher  $I_{MI}(p_i)$ , the more sensitive  $Q$  is to a variation of parameter  $p_i$ .

#### 4. Closed model results

Note to the reader: The main body of the manuscript is a very first draft. I already know that it is too verbose, contains confusing or tiring sections and has many other flaws. It should be seen as my first attempt to put thoughts on paper.

The results presented in this section are based on the data of 10000 simulations of the closed model (CM) which randomly sampled the parameter space as explained in Section 3, each yielding the equilibrium solution for a unique point in the parameter space provided in Table 1. The obtained dataset will henceforth be referred to as "CM data". The section is organised in two parts. First, we discuss basic features of the model and their implications for the partitioning of precipitation between land and ocean. Second, we examine to which parameters the precipitation ratio is most sensitive and which physical arguments explain the individual relationships.

##### a. Basic model behaviour

From a first visual inspection, it is clear that the equilibrium states and resulting equilibrium mean water fluxes  $P_l$ ,  $P_o$ ,  $E_l$ ,  $R$ ,  $A_l$  and  $A_o$ , show a strong dependence on the choice of land fraction  $\alpha$ . It is therefore instructive to discuss basic features of the model output with the help of scatter plots of the water fluxes over  $\alpha$ . These plots are provided in Figure 2. Similar figures that show the dependence on other parameters are provided in appendix [\*\*\*]. Note, that the ocean advection rate  $A_o$  has a negative value in all runs and is therefore multiplied by  $-1$  in order to obtain the absolute values which are more easily compared to the other fluxes.

All mean fluxes are functions of the equilibrium solutions to Eqns. (1) - (3) and therefore depend implicitly on the choice of parameter values. Expressions for the fluxes as explicit, analytical functions of  $\alpha$  or other parameters are cumbersome to find or may not exist. We therefore explain the observed features with qualitative, physical arguments rather than with mathematical rigor.

To begin with, Figure 2 shows that all equilibrium mean fluxes lie in the range  $[0, e_o]$ , with  $e_o \approx 3$  mm/day. With the exception of  $-A_o$ , maximum values are attained for  $\alpha \rightarrow 0$  and the fluxes

decrease monotonically but in nonlinear ways with increasing land fraction. To understand these general features and draw first conclusions for the partitioning of precipitation between land and ocean, two observations about the mean land advection rate  $A_1$  (bottom left panel) and runoff rate  $R$  (middle right panel) are key:

1. Land advection is positive (ocean advection is negative) for all equilibrium states.
2. The mean land advection rate is identical to mean runoff rate, i.e.  $A_1 = R$ .

The first observation implies a clear directionality of the atmospheric water transport for the system in equilibrium. Moisture is supplied *by* the ocean atmosphere *to* the land atmosphere. This directionality of advection sets the upper limit of the precipitation ratio in the following way: From Eq. (9) follows that a positive mean land advection rate requires the ocean atmosphere to be moister than the land atmosphere, i.e.  $w_o > w_l$ . As we assume that the same parametrization holds for precipitation over ocean and land, it further follows that  $P_o > P_l$  and, consequently,

$$PR = \frac{P_l}{P_o} < 1. \quad (13)$$

The second observation helps to explain why the unidirectionality of moisture transport from ocean to land exists. In order to sustain a constant, nonzero equilibrium soil moisture value,  $s > 0$ , land precipitation needs to balance the water loss of the soil through evapotranspiration and runoff. While the amount of precipitation that is turned into evapotranspiration resides in a self-sustaining recycling loop between land atmosphere and soil, runoff is irretrievably lost to the ocean. Its share in the precipitation balance needs to be supplied to the land atmosphere in the form of advection,

$$P_l = E_l + R = E_l + A_1. \quad (14)$$

If we imagine a system without advection, e.g. because the land and ocean atmosphere were separated by an impenetrable barrier, runoff would continuously reduce the soil moisture saturation and with it the evapotranspiration and precipitation fluxes. Eventually, the system would attain the trivial equilibrium solution  $\{s = 0, w_l = 0\}$ . On the ocean side of this hypothetical system, equilibrium conditions would be rather moist with  $w_o$  such that  $P_o(w_o) = e_o$ . We conclude that it

is the fundamental property of land to lose water in the form of runoff that requires an atmospheric moisture flux from ocean to land for any nontrivial equilibrium solution.

Based on these insights, we can also understand why no individual water flux can exceed the value of the ocean evaporation. Ocean precipitation needs to be smaller than  $e_o$  because some of the evaporated water gets advected by the land atmosphere and is no longer available for precipitation. Over land, we already established that  $P_l < P_o$  with the consequence that  $P_l < e_o$ . The land precipitation is partitioned into  $E_l$  and  $R$  so that each of these two fluxes must be smaller than  $e_o$ . Land advection is constrained by  $A_l = P_l - E_l < e_o$  and ocean advection is limited to  $A_o \lesssim e_o$  as the ocean atmosphere can only export as much moisture as it receives from the ocean surface minus the amount that precipitates. At the same time,  $A_o$  cannot attain  $e_o$  as the basic requirement for advection is  $w_o > w_l > 0$  which comes along with nonzero ocean precipitation.

As we increase the land fraction from  $\alpha = 0$  to  $\alpha = 1$ , all fluxes except  $A_o$  decrease in magnitude. The dependence of our system on  $\alpha$  enters our model equations through the mean advection rates  $A_l$  and  $A_o$ . The same amount of exchanged water per unit time  $(w_o - w_l)u$ , that solely depends on the atmospheric moisture contents and wind speed, translates to an amount per time and unit length for the ocean with factor  $1/((1 - \alpha)L)$  and for land with factor  $1/(\alpha L)$ . Combining Eqns. (2) and (3) under the equilibrium assumption of vanishing time derivatives, we can formulate the equilibrium condition,

$$e_o = P_o(w_o) + \frac{\alpha}{1 - \alpha} \underbrace{[P_l(w_l) - E_l(s)]}_{R(s)}. \quad (15)$$

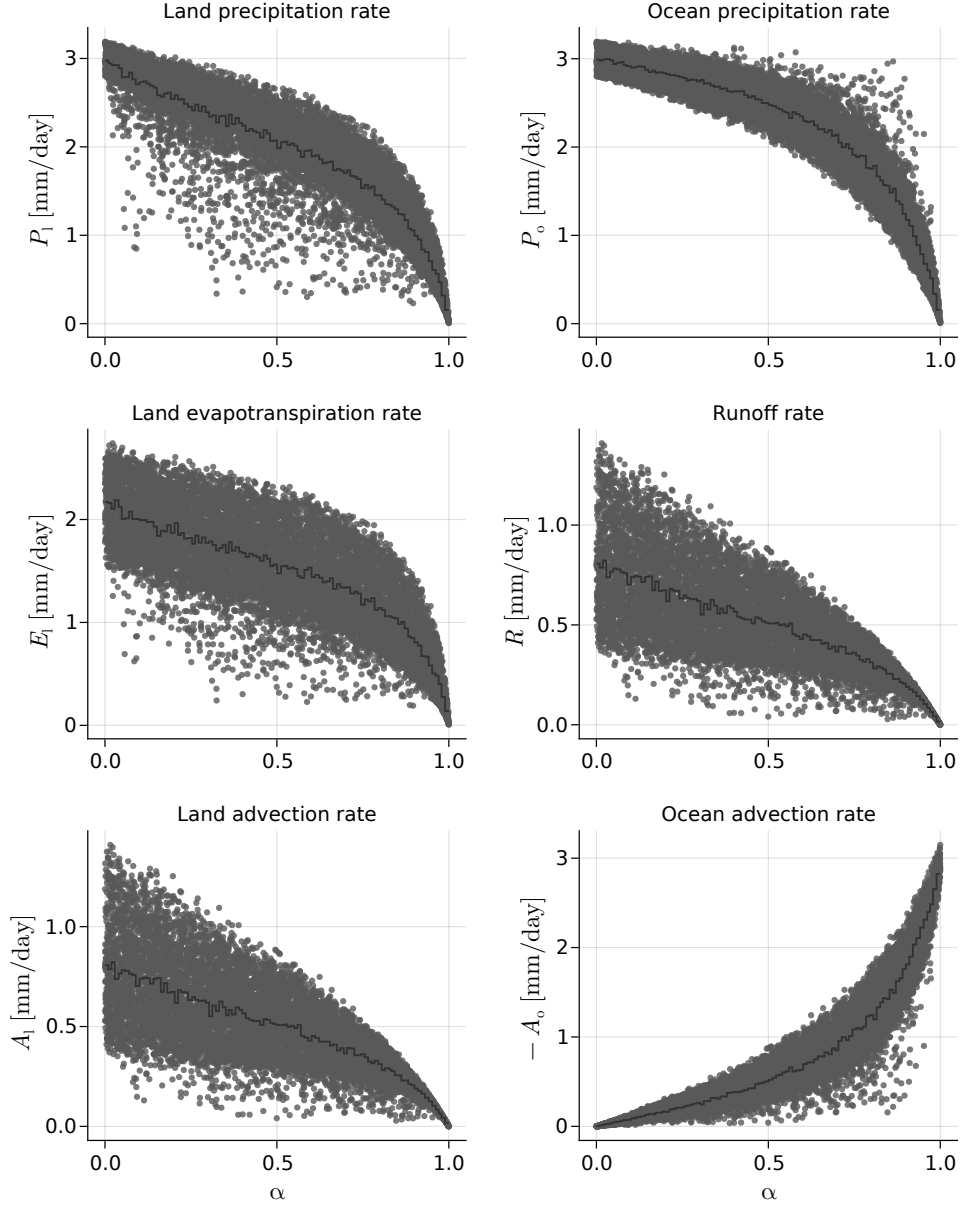
Equation (15) tells us, that the constant ocean evaporation rate needs to balance the sum of ocean precipitation rate and the difference between land precipitation and ET that is multiplied by an  $\alpha$ -dependent term. This term,  $\alpha/(1 - \alpha)$ , goes to zero for  $\alpha \rightarrow 0$  and increases monotonically until it diverges to infinity for  $\alpha \rightarrow 1$ . As  $\alpha$  increases, the equilibrium state needs to adjust by either decreasing  $w_o$ ,  $w_l$  or  $s$ . However, due to the coupling between all three state variables, a decrease in only one of the state variables does not result in a new equilibrium state. Instead, all state variables have to decrease together so that the new equilibrium state is dryer in all boxes (except the ocean). We can also understand this more intuitively: Despite the constant mean evaporation rate of the ocean, the total moisture input from the ocean is reduced as the land surface increases and the

ocean surface shrinks. A lesser amount of water is available to sustain the soil moisture value of a larger land box. Consequently, starting from a rather moist state when the ocean and its total water input into the atmosphere are large, the entire system undergoes drying with increasing land fraction. This process terminates when the entire model domain is covered by land ( $\alpha = 1$ ). Just before this point, when  $\alpha$  is close to 1, a tiny ocean atmosphere exports almost the entire moisture that gets evaporated from the ocean surface,  $(1 - \alpha)L|A_o| \lesssim e_o$ , but this amount is just sufficient to keep the large land atmosphere at a moisture value  $w_1 \gtrsim 0$  so that the resulting land precipitation stabilises the land at a very small soil moisture value  $s \gtrsim 0$ .

### b. Parameter sensitivity of $PR$

Building on the preceding general description of the model behavior, we now draw our attention to the sensitivity of the precipitation ratio with respect to a variation of different model parameters. Three parameters stand out in having a particularly strong impact on  $PR$ : Land fraction  $\alpha$ , atmospheric moisture transport parameter  $\tau$  and permanent wilting point  $s_{\text{pwp}}$ . We discuss the underlying relationships using the same CM data as before.

**Land fraction  $\alpha$ :** Figure 3 shows a scatter plot of  $PR$  values over  $\alpha$ . Despite considerable spread in  $PR$ , we can see that  $PR \rightarrow 1$  for both limits,  $\alpha \rightarrow 0$  and  $\alpha \rightarrow 1$ . This reflects very similar moisture conditions in the two atmospheres when  $\alpha$  is extreme. Knowing that  $w_o > w_1$  for all equilibrium states, it follows that  $PR$  will only decrease if  $\Delta w = w_o - w_1$  increases. As has been discussed in the preceding section, the system's equilibrium states for a tiny land domain are relatively moist. For  $\alpha \rightarrow 0$ , a large  $\Delta w$  cannot be sustained since the resulting advection amount  $\Delta w u$  would translate to a large land advection rate,  $\Delta w u / (\alpha L)$ , that would immediately moisten the land atmosphere and assimilate  $w_o$  and  $w_1$ . On the other end of the range, when the ocean is tiny, i.e.  $\alpha \rightarrow 1$ , large moisture differences are likewise impossible: This time,  $\Delta w$  is limited by the total amount of water that enters the system through the ocean surface. The ocean atmosphere cannot export more water than it receives. Therefore, the total amount of evaporated water sets the upper limit for advection,  $\Delta w u < (1 - \alpha)L e_o$ . This amount decreases with increasing  $\alpha$ , so that  $\Delta w$  needs to decrease with it. Moreover,  $\Delta w$  needs to stay below this limit since the ocean atmosphere has to stay moister than the land atmosphere to facilitate advection in the first place.



326 FIG. 2. Mean water fluxes computed from the equilibrium states of 10000 closed model runs with randomly  
 327 sampled parameter values and plotted over land fraction  $\alpha$ . The dark grey line shows the mean values of bins of  
 328 100 consecutive  $\alpha$ -values. The negative ocean advection rate  $A_o$  reflects a net transport of water out of the ocean  
 329 and into the land atmosphere. Multiplication by  $-1$  simplifies the comparison of its magnitude with the other  
 330 flux quantities.

351 Along the mid- $\alpha$  range,  $PR$  decreases until it reaches a minimum beyond which the ratio  
 352 increases again. This behaviour is somewhat concealed by the large spread in  $PR$  for intermediate



land fractions but is both visible in the means of bins of 100 consecutive  $\alpha$  values (dark grey line) and in graphs for which all parameters except  $\alpha$  were kept fixed (not shown). A mathematically rigorous analysis of  $PR(\alpha)$  in this range and, in particular, the location of the minimum is difficult due to the lack of an analytical expression for the relationship between precipitation ratio and land fraction. We can write,

$$PR(\alpha) = \frac{P_l(\alpha)}{P_o(\alpha)} = \frac{E_l(s) + \frac{(w_o - w_l)u}{\alpha L}}{e_o - \frac{(w_o - w_l)u}{(1-\alpha)L}}, \quad (16)$$

but we may not overlook the fact that our state variables are implicit functions of  $\alpha$ , too, i.e.  $s(\alpha)$ ,  $w_o(\alpha)$  and  $w_l(\alpha)$ . Even though we don't know the analytical form of these state variable dependencies, Eqn. (3) gives a useful indication of why the precipitation ratio should decrease for small but increasing  $\alpha$  and why it should increase again as  $\alpha$  approaches one. This indication lies in the factors  $f = 1/\alpha$  and  $g = 1/(1-\alpha)$  in the land and ocean advection rates, respectively. Assuming that the system resides in an equilibrium state for some  $\alpha$  close to zero, a small increase in  $\alpha$  would lead to a rather strong drop in the land advection rate (strong negative slope of  $f$  at low  $\alpha$ ) compared to the rather mild increase in the magnitude of ocean advection (weakly positive slope of  $g$  at low  $\alpha$ )...

I stopped here because I wondered if it makes sense to explain the shape of  $PR(\alpha)$  in such great detail. Maybe all this could be described in a much simpler way by starting from total moisture input rather than mean rates. The argument would go something like this: increasing land = generally less water available to the circulation in the system. Consequently, the moisture state as a whole must become drier, i.e. all state variables decrease but at different rates. Land precip (and with it  $w_l$ ) decrease both through a reduction of  $E_l$  and a rather sharp drop in  $A_l$  due to factor  $f$ . Ocean precip only decreases by slight increase of  $-A_o$ . For large  $\alpha$  the system is already in a rather dry state.  $E_l$  decreases only slightly with decreasing  $s$  and impact of  $f$  is less strong. For ocean precip, the opposite is true. Here,  $g$  plays a stronger role now and increases the ocean advection rate strongly. In the end, the interplay of the different nonlinear parametrisations make the behaviour of  $PR$  asymmetric around  $\alpha = 0.5$  and hard to understand in detail.

**Atmospheric rate of transport  $\tau$ :** The ratio between mean horizontal wind speed and spatial extent of the model,  $\tau = u/L$ , is a measure for the efficiency with which moisture is transported

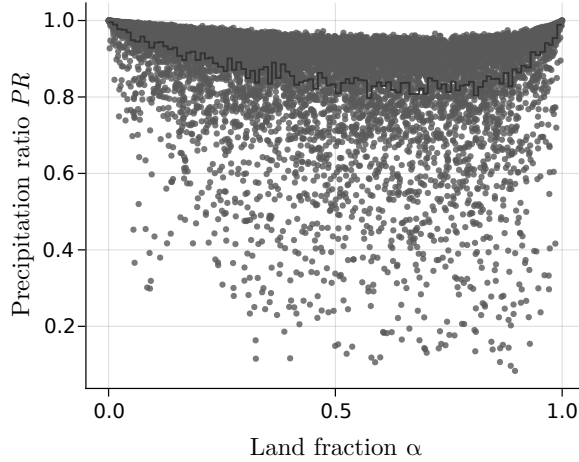


FIG. 3. Smile plot

across the model atmosphere. Its inverse value,  $\tau^{-1}$ , corresponds to the time that an air parcel would need to travel across the full domain length  $L$ . In the advection terms of Eqn. (2) and (3),  $\tau$  appears as the rate at which moisture is moved across the boundaries between the two atmospheric boxes. It has therefore major implications for the ability of advection to assimilate the moisture conditions over ocean and land. A very small value of  $\tau$ , i.e. a low rate of transport, corresponds to a combination of large domain size and low wind speed while a small domain and strong wind result in a very large value of  $\tau$ . Assuming a fixed land fraction  $\alpha$ , a larger moisture difference  $\Delta w$  is needed to move the same total amount of water across a box boundaries when the rate of transport is small, compared to when it is large. Except for the special cases of extreme land fractions,  $\alpha \rightarrow \{0, 1\}$ , where  $\alpha$  enforces very similar moisture conditions over land and ocean, it is primarily  $\tau$  that sets the moisture difference which is needed to attain the equilibrium state. This dominant role is illustrated in Figure 4 which shows the scatter plot of precipitation ratio over  $\tau$ . While we already assessed that  $\alpha$  sets the overall upper limit of  $PR$ , Fig. 4 shows that  $\tau$  sets the overall lower bound. It explains the large spread for  $PR$  values in the mid- $\alpha$  range in Figure 3, where the efficiency of atmospheric moisture transport is particularly important. Only high rates of transport enable the system to attain an equilibrium state with rather similar moisture conditions over land and ocean. For instance, if  $\tau > 0.4 \text{ day}^{-1}$ , then  $PR$  stays above 0.8 regardless of the choice of values for other parameters. Note, that  $\tau$  combines the information about both wind and spatial extent of the model. If one fixes one of the two, e.g.  $L = 40000 \text{ km}$  to simulate the full Tropics

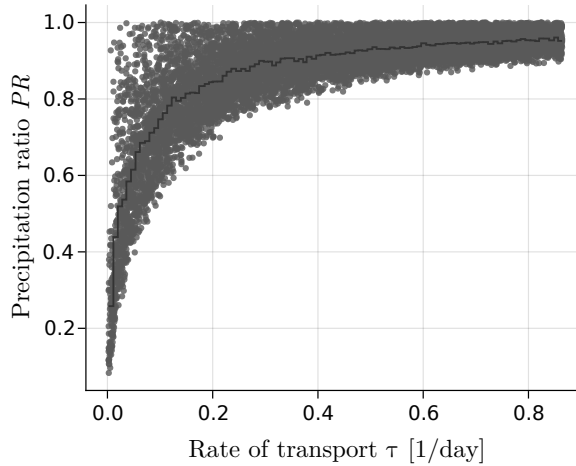


FIG. 4.  $\tau$ -dependence

399 along the equator, the physically sensible range of  $\tau$  is limited. For example, in order to obtain  
 400 a rate of transport larger than  $0.4 \text{ day}^{-1}$ , such a large  $L$  would require a minimum wind speed of  
 401  $185 \text{ m/s}$ , a value that lies beyond the highest wind speed ever measured on Earth. More realistic  
 402 mean wind speed values for such a large domain could lie around  $5$  to  $10 \text{ m/s}$  with corresponding  
 403 rates of transport,  $\tau \approx 0.01 - 0.02$ . At these low values of  $\tau$ , the spread of  $PR$  values is considerable  
 404 which means that also other parameters have a substantial influence on the attained equilibrium  
 405 state.

406 **Permanent wilting point  $s_{\text{pwp}}$ :** It takes work to extract water from the soil and the drier the soil,  
 407 the more work is needed to facilitate evapotranspiration. Regardless of whether the land surface  
 408 is bare or covered with vegetation,  $s_{\text{pwp}}$  is a characteristic property of the soil type which denotes  
 409 the relative soil moisture saturation value below which practically no water can be extracted.  
 410 The left panel of Figure 5 shows the parametrization function of evapotranspiration,  $E_1(s)$ , for  
 411 different choices of the permanent wilting point. For instance,  $s_{\text{pwp}} \approx 0.3$  might correspond to  
 412 loam and  $s_{\text{pwp}} \approx 0.5$  to clay (Hagemann and Stacke (2015)). In the evapotranspiration graphs,  
 413  $s_{\text{pwp}}$  determines the soil moisture value at which the curve transitions from  $E_1 \approx 0$  to the regime of  
 414 steeply increasing  $E_1$ . Since the field capacity  $s_{\text{fc}}$  lies  $\Delta s = 0.3$  higher than  $s_{\text{pwp}}$  for all relevant soil  
 415 types, a change in  $s_{\text{pwp}}$  merely shifts the evapotranspiration graph along the  $s$ -direction, while its  
 416 shape remains unchanged.

Figure 6 shows a negative trend of the precipitation ratio with increasing  $s_{\text{pwp}}$  for the performed model runs. The impact of soil type on the precipitation ratio is weaker than, for example, the impact of  $\tau$  but it is nonetheless clearly visible and  $s_{\text{pwp}}$  represents the third most sensitive model parameter. To understand the dependence of  $PR$  on  $s_{\text{pwp}}$ , it is convenient to think of a system in equilibrium for some permanent wilting point, e.g.  $s_{\text{pwp}} = 0.3$ . The mean equilibrium soil moisture value in the CM data for  $s_{\text{pwp}} = 0.3$  is  $s = 0.43$ . This initial state of the model is displayed as a blue dot in Figure 5. An abrupt increase of  $s_{\text{pwp}}$  to  $s_{\text{pwp}} = 0.4$  leads to a significant drop of  $E_1$  as illustrated by the first red arrow connecting the blue and green dot in the left panel of Fig. 5. The green dot represents a temporary state where the model is not in equilibrium because the state variables have not yet adapted to the new situation. At this point, the soil receives the same amount of precipitation but loses less water through evapotranspiration. As a result, the soil moistens. As time progresses, the system attains a new equilibrium state at a higher  $s$  value which is marked by the orange dot. This moistening of the soil is shown in the right panel of Fig. 5, where the equilibrium  $s$  values of the CM data are plotted over the corresponding values of  $s_{\text{pwp}}$ . However, as  $s$  increases, runoff and land advection rate increase, too. Assuming that  $\tau/(\alpha L)$  is kept fixed,  $\Delta w$  has to increase to facilitate the increase of advection. The water that is supplied to the land atmosphere as advection is taken from the ocean atmosphere, where  $w_o$  decreases as a consequence. Hence, an increase in advection is only possible, if  $w_l$  decreases more strongly than  $w_o$ . The increase in  $R$  combined with a decrease in  $P_l$  is the reason why the new equilibrium state for  $s_{\text{pwp}} = 0.4$  will have a moister soil but a lower evapotranspiration rate than the initial state for  $s_{\text{pwp}} = 0.3$ . The fact that  $w_l$  must decrease more strongly than  $w_o$  in the adaptation process is the reason why  $PR$  declines with increasing  $s_{\text{pwp}}$ .

## 5. Open model formulation

The closed model discussed so far can be applied to any system for which the total net advection is zero. Such conditions might be met in the real world when we look at very large scales, e.g. global domains such as the tropical band. However, in the case of more local, small scale phenomena, the net advection might not be zero and the situation is better captured by an open model configuration, where moisture inflow at the windward model boundary is a model parameter and no constraints apply to the moisture outflow at the leeward boundary. In this model configuration, the modelled

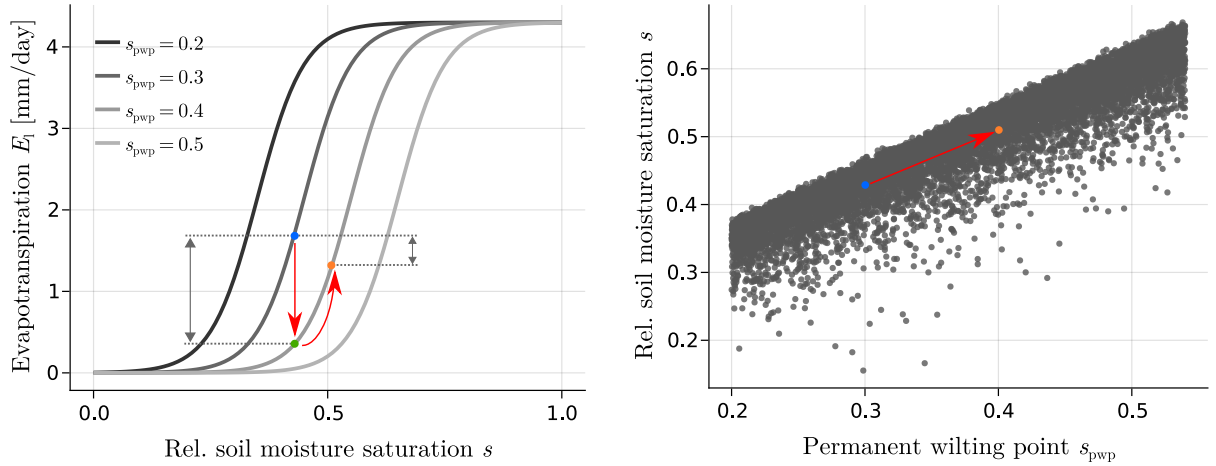


FIG. 5. Influence of an increase in  $s_{\text{pwp}}$  on the equilibrium state. Left: Higher values of  $s_{\text{pwp}}$  shift the graph of the  $E_l$  parametrization towards larger  $s$ . Right: Equilibrium values of the soil moisture saturation from CM data plotted over  $s_{\text{pwp}}$  values. In left panel, next to left black arrows will stand something like  $\Delta E_{\text{inst}}$  for instantaneous ET-difference and next to the right black arrows  $\Delta E_{\text{eq}}$  to denote the ET difference between old and new equilibrium state.

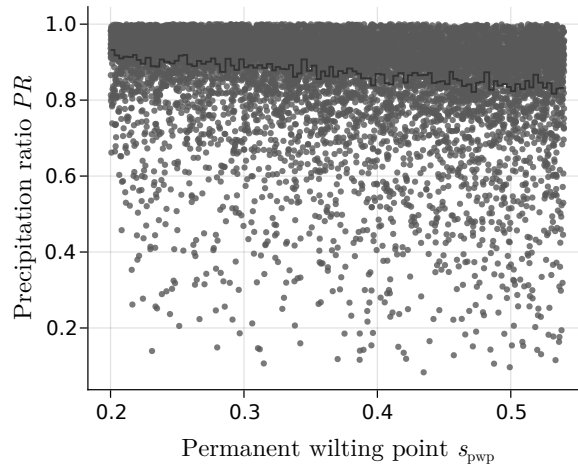


FIG. 6.  $s_{\text{pwp}}$ -dependence

domain can have a net advection larger or smaller than zero. In the following, we present the formalism and analysis of an open model with two oceanic domains and an island inbetween them.

453 *a. Open model equations*

454 The model equations for an open configuration are similar to the ones for the closed model. This  
 455 time, four instead of three equations are needed as the system has now one more ocean domain.  
 456 The meaning of the soil moisture variable  $s$  is unchanged, while a different notation is employed  
 457 for the water content of the atmospheric boxes. The index  $i = 1, 2, 3$  is used to denote the mean  
 458 integrated water vapour pass  $w_i$  and net advection rate  $A_i$  of the first ocean atmosphere ( $i = 1$ ),  
 459 land atmosphere ( $i = 2$ ) and second ocean atmosphere ( $i = 3$ ), respectively. With this, the model  
 460 equations read

$$\frac{ds}{dt} = \frac{1}{nz_r} [P(w_2) - R(s, w_2) - E(s)] \quad (17)$$

$$\frac{dw_1}{dt} = e_o - P(w_1) + A_1 \quad (18)$$

$$\frac{dw_2}{dt} = E(s) - P(w_2) + A_2 \quad (19)$$

$$\frac{dw_3}{dt} = e_o - P(w_3) + A_3, \quad (20)$$

461 with

$$A_i = \frac{(w_{i-1} - w_i)u}{L_i}. \quad (21)$$

462 Note, that a new parameter  $w_0$  was introduced which denotes the boundary condition of the water  
 463 vapor pass at the windward end of the model domain. It reflects the **synoptic scale?** conditions  
 464 which the model is embedded in.

465 *b. Open model results*

466

467 • How the open model relaxes the condition that  $PR < 1$  ( $PR > 1$  only under certain rare conditions)

468 • The role of synoptic moisture conditions in the atmosphere

469 • Open model can be transformed into the closed model

## 470 6. Discussion

471

- 472 • Which aspects of this study change the way we look at precipitation partitioning? (Especially,  
473 which relationships were not clear from the start?)
- 474 • Which conditions need to be met to end up with a precipitation ratio larger one, what role  
475 does a correct parametrization of precipitation play in this respect?
- 476 • What are possible use cases for the models?
- 477 • What can the model(s) tell us and what not and why? (e.g. land distribution not representative  
478 for the Tropics)
- 479 • ...

## 480 7. Conclusions

481 This study was motivated by our lack of theoretical understanding of how Earth's total pre-  
482 cipitation gets partitioned between land and ocean. More precisely, we wanted to know which  
483 physical processes and quantities determine the partitioning and whether the range of plausible  
484 values for these quantities sets constraints on the ratio between spatio-temporal mean land and  
485 ocean precipitation,  $PR = P_l/P_o$ .

486 To this end, we introduce a conceptual water balance model that describes the rate of change  
487 of soil moisture and atmospheric moisture over ocean and land, respectively. Drawing inspiration  
488 from earlier works by Rodriguez-Iturbe et al. (1991) and Bretherton et al. (2004), the water balance  
489 components are expressed as functions of the mean water content of the land and atmospheric  
490 subdomains. These functions contain several environmental parameters, some of which can be  
491 assumed to stay constant on human timescales, e.g. Earth's land fraction, and others that might  
492 change in a changing climate such as mean horizontal wind speed or properties of the soil.  
493 Assuming that the Earth system's moisture state is a steady state on the timescale of a couple of  
494 years, we analyze a large number of equilibrium solutions for different combinations of model  
495 parameter values. The obtained results can be summarized as follows:

- To reach equilibrium, the fundamental property of soil to lose water through runoff demands a net atmospheric moisture transport from the ocean to the land and a runoff return flow of identical magnitude from soil to ocean. In a closed, two-domain model, the ocean atmosphere will therefore equilibrate at a moister value than the land atmosphere. If the same relationship between precipitation and atmospheric moisture holds for land and ocean regions, then the precipitation ratio is bound by an upper limit of  $PR = 1$ .
- The lower bound of the precipitation ratio is mostly determined by the atmospheric moisture transport parameter,  $\tau = u/L$ . Efficient advection (large  $\tau$ ) results in similar moisture conditions over land and ocean and, hence, similar precipitation rates, while inefficient advection (low  $\tau$ ) leads to large moisture differences and an ocean precipitation up to ten times as strong as over land ( $PR \approx 0.1$ ). Significant sensitivity is also found to a variation of land fraction  $\alpha$  and to a lesser extent to the permanent wilting point and field capacity of the soil. The land fraction is most relevant near its extreme values of a large ocean and small land,  $\alpha \rightarrow 0$ , where the overall moisture state of the model is wet and of a small ocean and large land where the moisture state is dry. In both extreme cases, the precipitation ratio attains values close to one. In contrast, for intermediate values, the land fraction loses much of its predictive power and the influence of  $\tau$  dominates.
- The conceptual water balance model has difficulties explaining observed island precipitation enhancement. Although precipitation ratios larger than one are found for an open model configuration which is more apt for simulating the spatial scales of islands, these cases of precipitation enhancement make up for only a rather small subset of the parameter space which is characterized by small land sizes, rather large water vapor pass boundary values and a tendency for small values of  $\tau$ . A necessary condition for land precipitation enhancement in this model framework is a moisture cascade along the wind trajectory.

Although these findings suggest a rather strong and qualitatively robust sensitivity of precipitation partitioning to certain physical properties of the Earth system, we have to keep in mind that the employed model equations are the product of a number of strong assumptions. Foremost, we assumed the same precipitation parametrization to hold over land and ocean. It is likely that this is not justified. Knowing whether the same mean water vapour pass will result in more or



less precipitation over land compared to over ocean would clarify whether the precipitation ratio can become larger than one on global scales. An appropriate observational investigation of this relationship is therefore a possible direction for future studies. Another limitation of this study that might have a qualitative influence on the inferred bounds of the precipitation ratio is the role of land distributions. Configurations with more than one land box require additional model equations and will exhibit different equilibrium states for the same choice of model parameter values compared to the two-domain model configuration.

Lastly, the pure water balance approach explored in this study is insufficient to cover the full range of physical processes that are evoked by land-ocean differences. Especially the different ways in which the two surfaces partition incoming energy into sensible and latent heat fluxes might have a major indirect impacts on the partitioning of precipitation. For instance, it is plausible that sea breezes could temporarily transport more moisture into the land atmosphere, causing high rain rates due to the nonlinear dependence of precipitation on water vapor pass. In such a scenario, the ocean atmosphere could still be moister than the land atmosphere on average but mean precipitation over land might be higher even when using the same parametrization  $P(w)$ . Particularly in the context of island precipitation enhancement, energy considerations might be indispensable. Extending the model framework by energy balance equations or incorporating the effect of the diurnal cycle indirectly through energy-dependent parameters promises to yield a more complete theoretical understanding of precipitation partitioning.

544 *Acknowledgments.*

545 *Data availability statement.*

## 546 **References**

- 547 Bretherton, C. S., M. E. Peters, and L. E. Back, 2004: Relationships between water vapor path  
548 and precipitation over the tropical oceans. *J. Climate*, **17**, 1517–1528, [https://doi.org/10.1175/  
549 1520-0442\(2004\)017<1517:RBWVPA>2.0.CO;2](https://doi.org/10.1175/1520-0442(2004)017<1517:RBWVPA>2.0.CO;2).
- 550 Brubaker, K., D. Entekhabi, and P. Eagleson, 1991: Atmospheric water vapor transport: Estimation  
551 of continental precipitation recycling and parameterization of a simple climate model. URL  
552 <https://ntrs.nasa.gov/citations/19910018381>.
- 553 Brubaker, K. L., D. Entekhabi, and P. S. Eagleson, 1993: Estimation of continental precipita-  
554 tion recycling. *Journal of Climate*, **6**, 1077–1089, [https://doi.org/10.1175/1520-0442\(1993\)  
555 006<1077:EOCPR>2.0.CO;2](https://doi.org/10.1175/1520-0442(1993)006<1077:EOCPR>2.0.CO;2), URL [https://journals.ametsoc.org/jcli/article/6/6/1077/39303/  
556 Estimation-of-Continental-Precipitation-Recycling](https://journals.ametsoc.org/jcli/article/6/6/1077/39303/Estimation-of-Continental-Precipitation-Recycling).
- 557 Budyko, M. I., 1956: *Heat balance of the Earth's surface*. U.S. Dept. of Commerce, Weather  
558 Bureau.
- 559 Budyko, M. I., and O. A. Drozdov, 1953: Characteristics of the moisture circulation in the  
560 atmosphere. **4**, 5–14.
- 561 Burde, G. I., and A. Zangvil, 2001: The estimation of regional precipitation recycling. part i:  
562 Review of recycling models. *Journal of Climate*, **14** (12), 2497–2508, [https://doi.org/10.1175/  
563 1520-0442\(2001\)014<2497:TEORPR>2.0.CO;2](https://doi.org/10.1175/1520-0442(2001)014<2497:TEORPR>2.0.CO;2), URL [https://journals.ametsoc.org/jcli/article/  
564 14/12/2497/29526/The-Estimation-of-Regional-Precipitation-Recycling](https://journals.ametsoc.org/jcli/article/14/12/2497/29526/The-Estimation-of-Regional-Precipitation-Recycling).
- 565 Cronin, T. W., K. A. Emanuel, and P. Molnar, 2015: Island precipitation enhancement and  
566 the diurnal cycle in radiative-convective equilibrium. **141** (689), 1017–1034, [https://doi.org/  
567 10.1002/qj.2443](https://doi.org/10.1002/qj.2443), URL <https://rmets.onlinelibrary.wiley.com/doi/abs/10.1002/qj.2443>.
- 568 Datseris, G., 2018: Dynamicalsystems.jl: A julia software library for chaos and nonlinear dynam-  
569 ics. *Journal of Open Source Software*, **3**, 598, <https://doi.org/10.21105/joss.00598>.

- 570 Datseris, G., and U. Parlitz, 2022: *Nonlinear Dynamics*. 2192-4791, Springer International Pub-  
571 lishing, URL <https://link.springer.com/book/9783030910334>.
- 572 Eltahir, E. a. B., and R. L. Bras, 1994: Precipitation recycling in the amazon basin. *Quarterly Jour-*  
573 *nal of the Royal Meteorological Society*, **120**, 861–880, <https://doi.org/10.1002/qj.49712051806>,  
574 URL <https://onlinelibrary.wiley.com/doi/abs/10.1002/qj.49712051806>.
- 575 Ent, R. J. v. d., H. H. G. Savenije, B. Schaefli, and S. C. Steele-Dunne, 2010: Ori-  
576 gin and fate of atmospheric moisture over continents. *Water Resources Research*, **46** (9),  
577 <https://doi.org/10.1029/2010WR009127>, URL [https://agupubs.onlinelibrary.wiley.com/doi/abs/](https://agupubs.onlinelibrary.wiley.com/doi/abs/10.1029/2010WR009127)  
578 [10.1029/2010WR009127](https://doi.org/10.1029/2010WR009127).
- 579 Entekhabi, D., I. Rodriguez-Iturbe, and R. L. Bras, 1992: Variability in large-scale water bal-  
580 ance with land surface-atmosphere interaction. *Journal of Climate*, **5**, 798–813, [https://doi.org/](https://doi.org/10.1175/1520-0442(1992)005<0798:VILSWB>2.0.CO;2)  
581 [10.1175/1520-0442\(1992\)005<0798:VILSWB>2.0.CO;2](https://doi.org/10.1175/1520-0442(1992)005<0798:VILSWB>2.0.CO;2), URL [https://journals.ametsoc.org/](https://journals.ametsoc.org/jcli/article/5/8/798/35919/Variability-in-Large-Scale-Water-Balance-with-Land)  
582 [jcli/article/5/8/798/35919/Variability-in-Large-Scale-Water-Balance-with-Land](https://journals.ametsoc.org/jcli/article/5/8/798/35919/Variability-in-Large-Scale-Water-Balance-with-Land).
- 583 Fiedler, S., and Coauthors, 2020: Simulated tropical precipitation assessed across three major  
584 phases of the coupled model intercomparison project (CMIP). *Monthly Weather Review*, **148** (9),  
585 3653–3680, <https://doi.org/10.1175/MWR-D-19-0404.1>.
- 586 Findell, K. L., and E. A. B. Eltahir, 2003: Atmospheric controls on soil mois-  
587 ture–boundary layer interactions. part i: Framework development. *Journal of Hy-*  
588 *drometeorology*, **4** (3), 552–569, [https://doi.org/10.1175/1525-7541\(2003\)004<0552:](https://doi.org/10.1175/1525-7541(2003)004<0552:ACOSML>2.0.CO;2)  
589 [ACOSML>2.0.CO;2](https://doi.org/10.1175/1525-7541(2003)004<0552:ACOSML>2.0.CO;2), URL [https://journals.ametsoc.org/jhm/article/4/3/552/68951/](https://journals.ametsoc.org/jhm/article/4/3/552/68951/Atmospheric-Controls-on-Soil-Moisture-Boundary)  
590 [Atmospheric-Controls-on-Soil-Moisture-Boundary](https://journals.ametsoc.org/jhm/article/4/3/552/68951/Atmospheric-Controls-on-Soil-Moisture-Boundary).
- 591 Froidevaux, P., L. Schlemmer, J. Schmidli, W. Langhans, and C. Schär, 2014: Influence of  
592 the background wind on the local soil moisture–precipitation feedback. *Journal of the At-*  
593 *mospheric Sciences*, **71** (2), 782–799, <https://doi.org/10.1175/JAS-D-13-0180.1>, URL [https://](https://journals.ametsoc.org/doi/10.1175/JAS-D-13-0180.1)  
594 [journals.ametsoc.org/doi/10.1175/JAS-D-13-0180.1](https://journals.ametsoc.org/doi/10.1175/JAS-D-13-0180.1).
- 595 Hagemann, S., and T. Stacke, 2015: Impact of the soil hydrology scheme on simulated soil moisture  
596 memory. *Climate Dyn.*, **44**, 1731–1750, <https://doi.org/10.1007/s00382-014-2221-6>.

597 Hohenegger, C., P. Brockhaus, C. S. Bretherton, and C. Schär, 2009: The soil mois-  
 598 ture–precipitation feedback in simulations with explicit and parameterized convection. *Journal*  
 599 *of Climate*, **22** (19), 5003–5020, <https://doi.org/10.1175/2009JCLI2604.1>, URL [https://journals.](https://journals.ametsoc.org/jcli/article/22/19/5003/32298/The-Soil-Moisture-Precipitation-Feedback-in)  
 600 [ametsoc.org/jcli/article/22/19/5003/32298/The-Soil-Moisture-Precipitation-Feedback-in](https://journals.ametsoc.org/jcli/article/22/19/5003/32298/The-Soil-Moisture-Precipitation-Feedback-in).

601 Hohenegger, C., and B. Stevens, 2018: The role of the permanent wilting point in controlling the  
 602 spatial distribution of precipitation. *Proceedings of the National Academy of Sciences*, **115** (22),  
 603 5692–5697, <https://doi.org/10.1073/pnas.1718842115>, URL [https://www.pnas.org/content/115/](https://www.pnas.org/content/115/22/5692)  
 604 [22/5692](https://www.pnas.org/content/115/22/5692).

605 Lynn, B. H., W.-K. Tao, and P. J. Wetzel, 1998: A study of landscape-generated  
 606 deep moist convection. *Monthly Weather Review*, **126** (4), 928–942, [https://doi.org/](https://doi.org/10.1175/1520-0493(1998)126<0928:ASOLGD>2.0.CO;2)  
 607 [10.1175/1520-0493\(1998\)126<0928:ASOLGD>2.0.CO;2](https://doi.org/10.1175/1520-0493(1998)126<0928:ASOLGD>2.0.CO;2), URL [https://journals.ametsoc.org/](https://journals.ametsoc.org/mwr/article/126/4/928/66256/A-Study-of-Landscape-Generated-Deep-Moist)  
 608 [mwr/article/126/4/928/66256/A-Study-of-Landscape-Generated-Deep-Moist](https://journals.ametsoc.org/mwr/article/126/4/928/66256/A-Study-of-Landscape-Generated-Deep-Moist).

609 Manabe, S., 1969: CLIMATE AND THE OCEAN CIRCULATION: I. THE ATMOSPHERIC  
 610 CIRCULATION AND THE HYDROLOGY OF THE EARTH’S SURFACE. *Monthly Weather*  
 611 *Review*, **97** (11), 739–774, [https://doi.org/10.1175/1520-0493\(1969\)097<0739:CATOC>2.](https://doi.org/10.1175/1520-0493(1969)097<0739:CATOC>2.3.CO;2)  
 612 [3.CO;2](https://doi.org/10.1175/1520-0493(1969)097<0739:CATOC>2.3.CO;2), URL [https://journals.ametsoc.org/view/journals/mwre/97/11/1520-0493\\_1969\\_097\\_](https://journals.ametsoc.org/view/journals/mwre/97/11/1520-0493_1969_097_0739_catoc_2_3_co_2.xml)  
 613 [0739\\_catoc\\_2\\_3\\_co\\_2.xml](https://journals.ametsoc.org/view/journals/mwre/97/11/1520-0493_1969_097_0739_catoc_2_3_co_2.xml).

614 Peixóto, J. P., and A. H. Oort, 1983: The atmospheric branch of the hydrological cycle and  
 615 climate. *Variations in the Global Water Budget*, Springer Netherlands, 5–65, [https://doi.org/](https://doi.org/10.1007/978-94-009-6954-4_2)  
 616 [10.1007/978-94-009-6954-4\\_2](https://doi.org/10.1007/978-94-009-6954-4_2), URL [https://doi.org/10.1007/978-94-009-6954-4\\_2](https://doi.org/10.1007/978-94-009-6954-4_2).

617 Qian, J.-H., 2008: Why precipitation is mostly concentrated over islands in  
 618 the maritime continent. *Journal of the Atmospheric Sciences*, **65** (4), 1428–  
 619 1441, <https://doi.org/10.1175/2007JAS2422.1>, URL [https://journals.ametsoc.org/jas/article/65/](https://journals.ametsoc.org/jas/article/65/4/1428/26793/Why-Precipitation-Is-Mostly-Concentrated-over)  
 620 [4/1428/26793/Why-Precipitation-Is-Mostly-Concentrated-over](https://journals.ametsoc.org/jas/article/65/4/1428/26793/Why-Precipitation-Is-Mostly-Concentrated-over).

621 Rodriguez-Iturbe, I., D. Entekhabi, and R. L. Bras, 1991: Nonlinear dynamics of soil moisture at  
 622 climate scales: 1. stochastic analysis. *Water Resources Research*, **27**, 1899–1906, [https://doi.org/](https://doi.org/10.1029/91WR01035)  
 623 [10.1029/91WR01035](https://doi.org/10.1029/91WR01035).

Schär, C., D. Lüthi, U. Beyerle, and E. Heise, 1999: The soil–precipitation feedback: A process study with a regional climate model. *Journal of Climate*, **12** (3), 722–741, [https://doi.org/10.1175/1520-0442\(1999\)012<0722:TSPFAP>2.0.CO;2](https://doi.org/10.1175/1520-0442(1999)012<0722:TSPFAP>2.0.CO;2), URL <https://journals.ametsoc.org/jcli/article/12/3/722/28833/The-Soil-Precipitation-Feedback-A-Process-Study>.

Segal, M., and R. W. Arritt, 1992: Nonclassical mesoscale circulations caused by surface sensible heat-flux gradients. *Bulletin of the American Meteorological Society*, **73** (10), 1593–1604, [https://doi.org/10.1175/1520-0477\(1992\)073<1593:NMCCBS>2.0.CO;2](https://doi.org/10.1175/1520-0477(1992)073<1593:NMCCBS>2.0.CO;2), URL [https://journals.ametsoc.org/view/journals/bams/73/10/1520-0477\\_1992\\_073\\_1593\\_nmccbs\\_2\\_0\\_co\\_2.xml](https://journals.ametsoc.org/view/journals/bams/73/10/1520-0477_1992_073_1593_nmccbs_2_0_co_2.xml).

Seneviratne, S. I., T. Corti, E. L. Davin, M. Hirschi, E. B. Jaeger, I. Lehner, B. Orlowsky, and A. J. Teuling, 2010: Investigating soil moisture–climate interactions in a changing climate: A review. **99** (3), 125–161, <https://doi.org/10.1016/j.earscirev.2010.02.004>, URL <https://www.sciencedirect.com/science/article/pii/S0012825210000139>.

Shannon, C. E., 1948: A mathematical theory of communication. *The Bell System Technical Journal*, **27** (3), 379–423, <https://doi.org/10.1002/j.1538-7305.1948.tb01338.x>.

Sobel, A. H., C. D. Burleyson, and S. E. Yuter, 2011: Rain on small tropical islands. *Journal of Geophysical Research: Atmospheres*, **116**, <https://doi.org/10.1029/2010JD014695>, URL <https://agupubs.onlinelibrary.wiley.com/doi/abs/10.1029/2010JD014695>.

Ulrich, M., and G. Bellon, 2019: Superenhancement of precipitation at the center of tropical islands. *Geophysical Research Letters*, **46** (24), 14 872–14 880, <https://doi.org/10.1029/2019GL084947>, URL <https://agupubs.onlinelibrary.wiley.com/doi/abs/10.1029/2019GL084947>.

Wang, S., and A. H. Sobel, 2017: Factors controlling rain on small tropical islands: Diurnal cycle, large-scale wind speed, and topography. *Journal of the Atmospheric Sciences*, **74** (11), 3515–3532, <https://doi.org/10.1175/JAS-D-16-0344.1>, URL <https://journals.ametsoc.org/jas/article/74/11/3515/42168/Factors-Controlling-Rain-on-Small-Tropical-Islands>.

Zangvil, A., D. H. Portis, and P. J. Lamb, 1993: Diurnal variations in the water vapor budget components over the midwestern united states in summer 1979. *Interactions Between*

651 *Global Climate Subsystems*, American Geophysical Union (AGU), 53–63, [https://doi.org/](https://doi.org/10.1029/GM075p0053)  
652 10.1029/GM075p0053, URL <https://onlinelibrary.wiley.com/doi/abs/10.1029/GM075p0053>.